Diyala Journal of Engineering Sciences

ISSN 1999-8716
Printed in Iraq

Second Engineering Scientific Conference
College of Engineering –University of Diyala
16-17 December. 2015, pp. 538-545

INVESTIGATION ON OPTICAL AND ELECTRICAL PROPERTIES OF BILAYER GRAPHENE

Hamid. Toloue A.T[1], Bahar. Meshginqalam[2], Ahmed. K. Jameil [3], Mohammad. Taghi. Ahmadi[*4], Anthony Centeno[5]

[1] PhD student- Nano i-kohza, Malaysia- Japan International Institute of Technology (MJIIT), Universiti Teknologi Malaysia, Malaysia- h.toloue@gmail.com
[2] PhD student - Physics Department, Faculty of Sciences, Urmia University, Urmia, Iran- bahar.meshginqalam@gmail.com
[3] Department of Computer and Software Engineering, College of Engineering, Diyala University, Iraq, ahmedkhudaer@yahoo.com
[4*] Assistant Professor ,Nanotechnology Research Center, Nano electronic Research Group, Physics Department, Urmia University, Urmia, Iran- ahmadiph@gmail.com
[5] Associate Professor - Nano i-kohza, Malaysia- Japan International Institute of Technology (MJIIT), Universiti Teknologi Malaysia, Malaysia- acenteno@ic.utm.my

ABSTRACT: - In this paper, a theoretical study on the optical and electrical properties of bilayer graphene is presented. Graphene with a single atomic layer of carbon and outstanding optical properties is an ideal nominee on sensor application because of high surface-to-volume ratio. In this report optical properties of bilayer graphene nanoribbon (BGN) in the presence of applied bias for different incident wavelength are explored. (BGN) dielectric constant and refractive index based on its conductance are modeled theoretically and obtained results are simulated numerically. Based on the presented model applied bias effect on BGN optical parameters are discussed.

These results are relevant for applications of recently developed graphene based devices in advanced optoelectronics such as surface plasmon resonance sensors.

Key words: optical property, graphene, refractive index, bilayer graphene, model

1. INTRODUCTION

Two dimensional (2D) honeycomb lattice of graphene [1] has exclusive optoelectronic properties with enormous application potential on future nanoscale devices[2-4]. Its band energy is a major factor which plays a significant role on carrier transport has been explored widely [5-8]. In contrast with graphene nanoribbon, bilayer graphene nanoribbon (BGN) consists of two Bernal AB stacked layers which is shown in figure (1).

Bilayer graphene nanoribbon (BGN) with unique optical and electrical properties has been studied in different nanoscale fields such as field effect transistors (FETs) and schottky diodes [9-11].However increasing industrial and clinical demand on graphene based optical devices such as surface plasmon resonance (SPR) sensors requires its optical properties to be explored [12-16]. In this paper optical properties of bilayer graphene nanoribbon (BGN) in the presence of applied voltage for different incident wavelength are explored. (BGN) dielectric constant and refractive index based on its conductance are modeled theoretically and obtained results are simulated numerically. Applied bias effect on BGN optical parameters are discussed based on the presented model. Moreover these results are applicable in advanced graphene based optoelectronic devices such as surface plasmon resonance sensors.

2. MODEL

Conductance is one of the main parameters which need to be discovered then the optical properties of BNG can be derived from conductance in specific condition. First step to analyze conductance is started with parabolic band energy approximation. For the proposed BGN, the tight-binding technique is adopted in order to calculate the energy band structure of BGN with AB stacking [17]:

$$E_{k(V)} = \pm\sqrt{\varepsilon_k^2 + \frac{t_\perp^2}{2} + \frac{V^2}{4} \pm \sqrt{(t_\perp^2 + V^2)\varepsilon_k^2 + \frac{t_\perp^2}{4}}}, \qquad (1)$$

Where V is the applied voltage, $t_\perp$ is the interlayer hopping energy, ε_k^2 is derived from the below equation which is clear that it is depends on applied voltage and interlayer hopping energy.

$$\varepsilon_k^2 = \frac{(\frac{V^4}{4} + \frac{V^2 t_\perp^2}{2})}{(V^2 + t_\perp^2)}, \qquad (2)$$

Energy equation (Eq. (1)) can be exposed as:

$$E_{(k)} \approx \Delta - \alpha k^2 + \beta k^4, \qquad (3)$$

Where $\Delta = V/2$, $k = 2\pi n/\lambda$, is the wave vector, α and β coefficients are depends on the value of Fermi velocity. $\alpha = (\frac{V}{t_\perp^2})v_F^2$, $\beta = \frac{v_F^4}{Vt_\perp^2}$ Fermi velocity is defined by $v_F = \frac{3ta_{c-c}}{2\hbar}$.

Where a_{c-c} is the lattice spacing which is equal to $1.4\,\mathring{A}$. In addition based on conductance definition (G=I/V), the Boltzmann transport equation can be written as the Landauer formula which illustrates conductance with Ohmic behavior, parabolic band energy directs to number of mode calculation. However in the smaller length the interface resistance and width effect in the form of number of modes are considered as:

$$G = \frac{2q^2}{h}\int_{-\infty}^{+\infty} M(E)T(E)\left(-\frac{df}{dE}\right)dE \qquad (4)$$

Where q is the electron charge, T is transmission probability which is equal to one in ballistic limit, h is the Planck's constant, M is the number of modes and f is the Fermi–Dirac distribution function. Furthermore one dimensional quantum confinement effect demonstrates temperature-dependent conductance with minimum value near the Dirac point that proves Fermi-Dirac integral based method on conductance expression. The general mathematical model of conductance for BGN, which can be solved numerically is written here [17].

$$G_{BGN} = -\frac{4q^2}{hl}\int_{-v_g}^{+v_g}\left(\frac{1}{1+e^{\left(x-\frac{(v_g-v)q}{k_BT}\right)}}\right)\left(\frac{3}{4}\sqrt{\frac{a+\sqrt{a^2+4\beta x k_BT}}{2\beta\left(a^2+4\beta x k_BT\right)}} - \frac{a}{8\beta\left(a^2+4\beta x k_BT\right)\sqrt{\frac{a+\sqrt{a^2+4\beta x k_BT}}{2\beta}}}\right)dx \qquad (5)$$

Where V is the biased voltage, v_g is the gate voltage, k_B is the boltzmann constant, T is temperature and x = (E − Δ)/k_BT. Furthermore, Fermi-Dirac general integral forms conductance needs to be recognized by role of degeneracy. An acceptable agreement with previous experimental result achieved by comparing with common form of conductance based on the presented model in the ballistic limit which is shown in figure 2.

3. RESULT AND DISCUSSION

The conductivity equation is applied to explore the BGN optical parameters such as complex refractive index. Electrical conductance is almost equal to optical conductance by applied weak electromagnetic field[18]. By applying the conductance equation, the current density per cross section area is modified as:

$$J=-\frac{4q^2E}{\delta hl}\int_{-v_g}^{+v_g}\left(\frac{1}{1+e^{\left(x-\frac{(v_g-v)q}{k_BT}\right)}}\right)\left(\frac{3}{4}\sqrt{\frac{a+\sqrt{a^2+4\beta xk_BT}}{2\beta\left(a^2+4\beta xk_BT\right)}}-\frac{a}{8\beta\left(a^2+4\beta xk_BT\right)\sqrt{\frac{a+\sqrt{a^2+4\beta xk_BT}}{2\beta}}}\right)dx \qquad (6)$$

Where thickness of BGN is δ and $E'=E'_0e^{+i\omega t}$ is the electric field vector. Together with Ampere's current law, conductance is employed to calculate the dielectric function of BGN.

$$\frac{G}{\delta}E_0e^{i\omega t}+i\omega\varepsilon_0E_0e^{i\omega t}=i\omega\varepsilon_0\varepsilon_gE_0e^{i\omega t} \qquad (7)$$

Where ε_0 is the vacuum permittivity, ω is the frequency and ε_g is the bilayer graphene dielectric constant. From which we can extract the relative dielectric constant that presents conductance resembling trends in dielectric constant expression.

$$\varepsilon_g=\frac{G}{i\delta\omega\varepsilon_0}+1 \qquad (8)$$

By considering the wide application of degenerate regime in nanoscale devices, equation (5) was analytically solved [17]. In degenerate limit, number of carriers increases rapidly and probability of occupied energy levels is equal to one, therefore the dielectric function as a function of BGN geometry is:

$$\varepsilon_g=\frac{G_{BGN}^D}{i\,\delta\omega\varepsilon_0}+1=\frac{q^2}{\sqrt{2}ihl\,\varepsilon_0\omega K_BT\,\delta}\left(\sqrt{\left(\frac{a+\sqrt{a^2+4\beta xk_BT}}{\beta}\right)^3}-\frac{\alpha}{\beta}\sqrt{\frac{a+\sqrt{a^2+4\beta xk_BT}}{\beta}}\right)\Bigg|_{-v_g}^{v_g}+1 \qquad (9)$$

In non-equilibrium conditions, conductance as a function of applied voltage has been reported [19-21]. Analytical model illustrates same performance on dielectric function as shown in figure 3. In other word dielectric function is changed by applied voltage together with wavelength variation.

By increasing the applied voltage the imaginary part of dielectric constant of BGN decreases (absorption increased as absolute value increased) but the real part remains constant. The conductance per atomic layer in mass less Dirac fermium band structure is a universal constant that directs to atomic layer dependent refractive index, in agreement with the theoretical anticipation on atomic density as[22, 23]. The degenerate condition plays dominant rule as the BGN shrinks to the nanoscale regime and universal conductance can be used in calculation of BGN optical properties.

$$G=-\frac{q^2}{\sqrt{2}hlK_BT}\left(\sqrt{\left(\frac{a+\sqrt{a^2+4\beta xk_BT}}{\beta}\right)^3}-\frac{\alpha}{\beta}\sqrt{\frac{a+\sqrt{a^2+4\beta xk_BT}}{\beta}}\right)\Bigg|_{-v_g}^{v_g}\approx\frac{q^2}{4\hbar}\approx 6.08\times10^{-5}(\Omega^{-1}) \qquad (10)$$

The normalization will affect the universal conductance therefore it will be independent of unit system consequently the refractive index is simplified as:

$$n_g = \sqrt{\varepsilon_g} = \sqrt{\frac{G_{BGN}^{D}}{i\delta\omega\varepsilon_0} + 1} \tag{11}$$

Subsequently the effect of applied bias on refractive index illustrated in figure 4. Additionally refractive index as a function of wavelength is explored:

$$n_g = \sqrt{\frac{G_{BGN}^{D}}{i2\pi c\delta\varepsilon_0}\lambda + 1} \tag{12}$$

The real part of refractive index accounts for refraction while the imaginary part leads to absorption. The real part of n is increased by increasing the applied voltage and wave length but for the imaginary part of n it is vice versa [22]. Additionally it is confirmed that, real part of modeled refractive index is increased while the imaginary part of it, is decreased by increasing wave length for different voltages as shown in figure (5).

Consequently refractive index is increased by growth of applied bias on BGN. It can be concluded that real and imaginary parts of refractive index can be engineered by controlled applied voltage. Possibility of BGN application under controlled bias as a gold replacement on optical sensors needs to be explored in future work.

4. CONCLUSION

Graphene based materials demonstrate outstanding mechanical, electrical and optical features which make them hopeful materials for future optoelectronic devices. Moreover determination of optical and electrical properties of bilayer graphene is necessary for graphene based optical sensors investigations such as graphene based surface plasmon resonance sensors. Furthermore tunable optical properties can lead to better sensor performances. In the presented research optical conductance of bilayer graphene in the calculation of dielectric constant and refractive index is employed. The controllable BGN dielectric constant by incident wave length and applied voltage is rendered. Consequently applied voltage and wave length dependent tunable refractive index is reported in the degenerate condition based on the conductance model. Thus the possibility of BGN application as a gold replacement in surface plasmon resonance based sensors under controlled bias is suggested.

REFERENCES

1) Gosciniak, J. and D.T.H. Tan, Theoretical investigation of graphene-based photonic modulators. Sci. Rep., 2013. 3.
2) Costamagna, S. and A. Dobry, From graphene sheets to graphene nanoribbons: Dimensional crossover signals in structural thermal fluctuations. Physical Review B, 2011. 83(23).
3) Dean, C., et al., Graphene based heterostructures. Solid State Communications, 2012. 152(15): p. 1275-1282.
4) Luican, A., et al., Single-Layer Behavior and Its Breakdown in Twisted Graphene Layers. Physical Review Letters, 2011. 106(12).
5) Abergel, D.S.L., et al., Properties of graphene: a theoretical perspective. Advances in Physics, 2010. 59(4): p. 261-482.
6) Adonkin, V.T., et al., EFFECT OF INTERCALATION AND EXFOLIATION ON POSITRON-ANNIHILATION LIFETIMES IN GRAPHITES. Journal of Physics and Chemistry of Solids, 1994. 55(5): p. 443-446.
7) Akdim, B. and R. Pachtert, Switching Behavior of Carbon Chains Bridging Graphene Nanoribbons: Effects of Uniaxial Strain. Acs Nano, 2011. 5(3): p. 1769-1774.

8) Elias, D.C., et al., Control of Graphene's Properties by Reversible Hydrogenation: Evidence for Graphane. Science, 2009. 323(5914): p. 610-613.
9) Paul, M.J., et al., High-field terahertz response of graphene. New Journal of Physics, 2013. 15(8): p. 085019.
10) Sadeghi, H., et al., CARRIER STATISTICS MODEL FOR A BILAYER GRAPHENE NANORIBBON IN THE NONDEGENERATE REGIME, in Proceedings of the Fourth Global Conference on Power Control and Optimization, N.W.J.F.V.P. Barsoum, Editor. 2011. p. 184-187.
11) Rahmani, M., et al., Performance of Bilayer Graphene Nanoribbon Schottky Diode in Comparison with Conventional Diodes. Journal of Computational and Theoretical Nanoscience, 2013. 10(2): p. 323-327.
12) Afzali, A., et al., Optical sensor useful for determining makeup of any analyte that acts to shift peak surface plasmon resonance (SPR) of graphene, comprises a substrate, and a sensing surface comprising a graphene layer located on the substrate. Egypt Nanotechnology Cent; Int Business Machines Corp.
13) Acik, M. and Y.J. Chabal, Nature of Graphene Edges: A Review. Japanese Journal of Applied Physics, 2011. 50(7).
14) Huang, Y., et al., Nanoelectronic biosensors based on CVD grown graphene. Nanoscale, 2010. 2(8): p. 1485-1488.
15) Phan, A.D. and N.A. Viet, A new type of optical biosensor from DNA wrapped semiconductor graphene ribbons. Journal of Applied Physics, 2012. 111(11).
16) Huang, Y., et al., Graphene-based biosensors for detection of bacteria and their metabolic activities. Journal of Materials Chemistry, 2011. 21(33): p. 12358-12362.
17) Hatef, S., et al., Bilayer Graphene Nanoribbon Transport Model, in Advanced Nanoelectronics. 2012, CRC Press. p. 203-222.
18) Singh, R.J., Solid State Physics. 2012: Dorling Kindersley.
19) Sadeghi, H., et al., CHANNEL CONDUCTANCE OF ABA STACKING TRILAYER GRAPHENE NANORIBBON FIELD-EFFECT TRANSISTOR. Modern Physics Letters B, 2012. 26(8).
20) Amin, N.A., et al., DRIFT VELOCITY AND MOBILITY OF A GRAPHENE NANORIBBON IN A HIGH MAGNITUDE ELECTRIC FIELD, in Proceedings of the Fourth Global Conference on Power Control and Optimization, N.W.J.F.V.P. Barsoum, Editor. 2011. p. 177-179.
21) Dellabetta, B. and M.J. Gilbert, The Effect of Disorder in Superfluid Graphene Bilayers. 2010 14th International Workshop on Computational Electronics, ed. G. Basso and M. Macucci. 2010. 57-60.
22) Min, S.K., et al., Theoretical Design of Nanomaterials and Nanodevices: Nanolensing, Supermagnetoresistance, and Ultrafast DNA Sequencing. Journal of Physical Chemistry C, 2011. 115(33): p. 16247-16257.
23) Velasco, J., Jr., et al., Quantum transport in double-gated graphene devices. Solid State
24) Ahmadi, M.T., et al., Graphene Nanoribbon Conductance Model in Parabolic Band Structure. Journal of Nanomaterials, 2010.

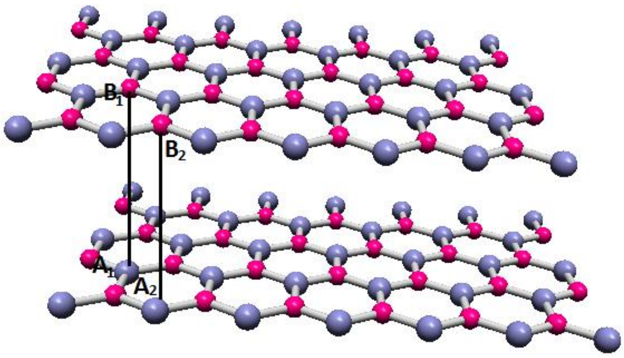

Figure(1): The schematic of bilayer graphene nanoribbon (AB-stacked configuration)

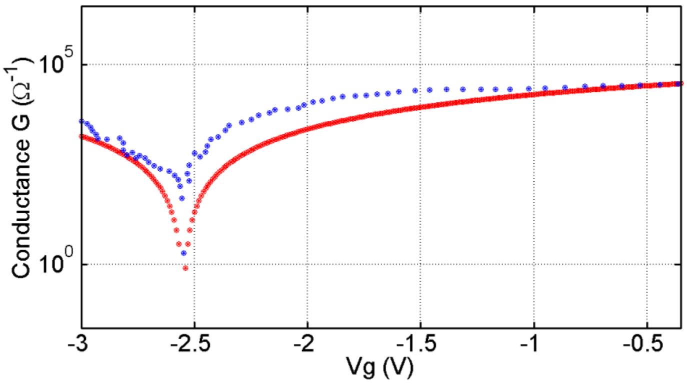

Figure (2): BGN conductance model in comparison with experimental data [24]

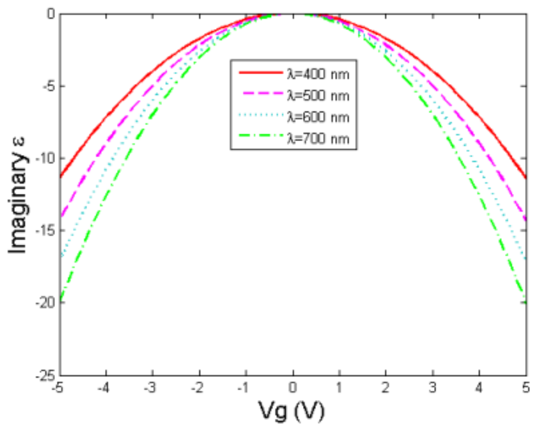

Figure (3): The effect of non-equilibrium condition on the dielectric function with different wavelengths that shows bias dependence optical parameters on BNG.

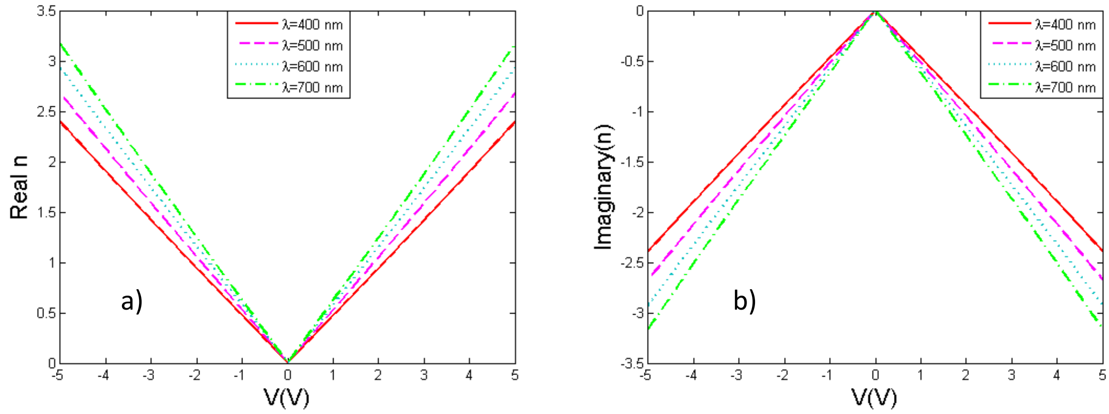

Figure (4): a) Applied bias effect on real part of refractive index   b) Applied bias effect on imaginary part of refractive index both for different wave lengths

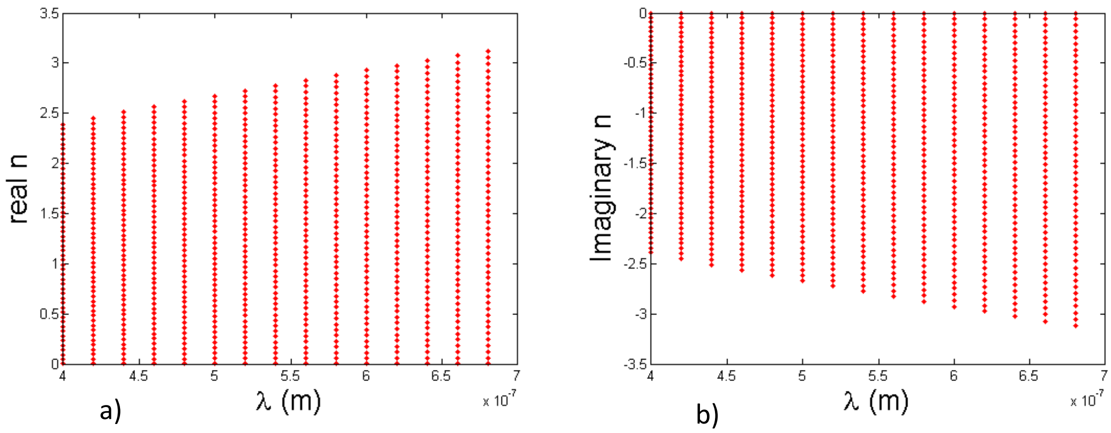

Figure (5): a) The wave length increment effect on real part of refractive index   b) The wave length decrement effect on imaginary part of refractive index in degenerate condition with applied bias

التحقيق في الخصائص البصرية للطبقة ثنائية الجرافين

حميد طلوع، بهار مشكين قلم، احمد خضير جميل ، محمد تقي احمدي *، آنتونى سنتنو

الخلاصة:

في هذا البحث ، قدمت الدراسة النظرية على الخصائص البصرية والكهربائية للطبقة ثنائية الجرافين. الجرافين مع طبقة واحدة ذرية من الكربون والخصائص البصرية المعلقة هو المرشح المثالي على تطبيق الاستشعار بسبب نسبة عالية السطح إلى الحجم. في هذا التقرير يتم استكشاف الخصائص البصرية ل nanoribbon طبقة ثنائية الجرافين (BGN) في وجود تحيز بطلب للحصول على مختلف الطول الموجي الحادث. وعلى غرار (BGN) مؤشر المستمر والانكسار عازلة على أساس تصرف لها نظريا والحصول على محاكاة النتائج عدديا. استنادا إلى النموذج المقدم تطبيق تأثير التحيز على اجزاء البصرية BGN التي يتم مناقشتها. هذه النتائج ذات الصلة للتطبيقات وضعت مؤخرا أجهزة الجرافين مقرها في الإلكترونيات الضوئية المتطورة مثل أجهزة الاستشعار الرنين لتأكل السطح.